Structure–Function Relationship in Glaucoma Patients With Parafoveal Versus Peripheral Nasal Scotoma

Kyoung In Jung,[1] Min Ku Kang,[1] Jin A. Choi,[2] Hye-Young Shin,[3] and Chan Kee Park[1]

[1]Department of Ophthalmology and Visual Science, Seoul St. Mary's Hospital, College of Medicine, Catholic University of Korea, Seoul, Korea
[2]St. Vincent's Hospital, Department of Ophthalmology, College of Medicine, Catholic University of Korea, Seoul, Korea
[3]Uijeongbu St. Mary's Hospital, Department of Ophthalmology, College of Medicine, Catholic University of Korea, Seoul, Korea

Correspondence: Chan Kee Park, Department of Ophthalmology and Visual Science, Seoul St. Mary's Hospital, College of Medicine, Catholic University of Korea, 505 Banpo-dong, Seocho-ku, Seoul 137-701, Korea;
ckpark@catholic.ac.kr.

Submitted: September 24, 2015
Accepted: December 31, 2015

Citation: Jung KI, Kang MK, Choi JA, Shin H-Y, Park CK. Structure–function relationship in glaucoma patients with parafoveal versus peripheral nasal scotoma. *Invest Ophthalmol Vis Sci.* 2016;57:420–428. DOI:10.1167/iovs.15-18256

Purpose. We evaluated whether the structure–function relationship in glaucoma patients with parafoveal scotoma or peripheral scotoma differs with the use of frequency doubling technology (FDT) or short-wavelength automated perimetry (SWAP) compared to standard automated perimetry (SAP).

Methods. Glaucoma patients with isolated parafoveal scotoma (PFS) within the central 10° of fixation in 1 hemifield and those with an isolated peripheral nasal step (PNS) within the nasal periphery outside 10° of fixation in one hemifield were studied. Peripapillary retinal nerve fiber layer (RNFL) thickness was measured using spectral-domain optical coherence tomography. The topographic relationships between structure and function were investigated.

Results. In the PNS group, superotemporal ($r^2 = 0.300$, $P = 0.001$) and inferotemporal ($r^2 = 0.302$, $P = 0.001$) RNFL thickness showed significant correlations with the corresponding visual field (VF) sensitivity using linear regression model in SAP. In the PFS group, temporal RNFL thickness was not correlated with nasal mean sensitivity (MS) on SAP ($r^2 = 0.103$, $P = 0.065$). Using FDT, however, the temporal RNFL thickness was correlated with nasal MS in the PFS group ($r^2 = 0.277$, $P = 0.001$). Using SWAP, the temporal RNFL thickness was not significantly associated with regional VF sensitivity in the PFS group ($r^2 = 0.052$, $P = 0.192$).

Conclusions. In glaucoma with peripheral scotoma, the RNFL thickness was associated significantly with the corresponding VF loss in SAP, FDT, and SWAP. In eyes with PFS, however, the topographic structure–function relationships were not distinct with SAP or SWAP. Frequency doubling technology performed well in terms of structure–function correlation in glaucoma with PFS.

Keywords: frequency doubling technology, parafoveal scotoma, short-wavelength automated perimetry, standard automated perimetry, structure–function relationship

Structural damage is thought commonly to precede functional loss in glaucoma.[1] Quigley et al.[2,3] and Anderson[4] suggested that many retinal ganglion cells (RGCs) could be lost before conventional visual field (VF) tests detect a defect. That is, standard automated perimetry (SAP) may detect the glaucoma only after the death of a large number of RGCs, even though SAP still is the gold standard for the functional analysis of glaucoma.[5–7]

Several "unconventional" perimetry methods have been evaluated in many studies, which demonstrated their ability to detect the early glaucoma; for example, short-wavelength automated perimetry (SWAP) and frequency doubling technology perimetry (FDT).[5]

Numerous studies have reported that the FDT shows good sensitivity and specificity for detecting glaucoma.[6–8] Frequency doubling technology perimetry may detect the development of VF defects earlier and performs as well as, if not better than, SAP for detecting glaucomatous VF defects.[9–15] The introduction of the second generation of FDT, Matrix FDT perimetry, enhanced the spatial resolution by using a 24-2 strategy similar to SAP.[15] Test–retest variability of VF by SAP is greater within and near glaucomatous VF defects than to regions with normal sensitivity.[16–18] Increased variability with reductions in sensitivity is not present for frequency-doubling perimetry.[18–23]

Studies indicate that SWAP testing found early glaucomatous damage and that the test may indicate significant change in visual function before it is apparent on standard white-on-white VFs, although its weakness is greater long-term fluctuation and more learning effect artifact compared to SAP.[5,24–28] A new generation of SWAP techniques uses more efficient strategies, the Swedish interactive threshold algorithm (SITA), to reduce testing time. The SITA SWAP testing shows higher sensitivities than full-threshold SWAP dose, although there are controversies about that.[29–31]

Mean sensitivity (MS) of SAP is highest centrally and gradually decreases toward the periphery.[32] Landers et al.[32] reported that the topography of the FDT field is flatter than SAP fields, and that of the SWAP fields was steeper than SAP. Therefore, the structure–function relationship in glaucoma patients with parafoveal scotoma or peripheral scotoma may differ with the use of unconventional VF tests compared to SAP.

Investigative Ophthalmology & Visual Science

A paracentral scotoma is important because central visual disturbance may put patients at greater risk of losing visual acuity, leading to lower driving performance.[33–35] Given the fact that central vision is clinically important, an accurate assessment of visual function in macular region is critical. In this study, we investigated whether the structure–function relationships in glaucoma patients with initial paracentral scotoma and initial peripheral scotoma differ among three types of perimetry; that is, SAP, FDT, and SWAP. Comparison of these types of perimetry in two distinct patterns of scotoma may be helpful in clarifying the structure–function relationship and appropriate clinical application of VF tests in glaucoma, especially with paracentral scotoma.

Methods

This investigation was approved by the Institutional Review Board of the Catholic University of Korea, Seoul, Korea, and followed the tenets of the Declaration of Helsinki. Patients with glaucoma that met the inclusion criteria were consecutively included from patients examined for glaucoma at the glaucoma clinic of Seoul St. Mary's Hospital between March 2013 and December 2013.

Inclusion criteria were best-corrected visual acuity of 20/40 or better, spherical equivalent within ±7 spherical diopters (D) and ±3 D cylinder. The inclusion criteria were eyes with a normal open angle, and the presence of a glaucomatous optic disc, such as diffuse or focal rim thinning, notching, optic disc hemorrhage, retinal nerve fiber layer (RNFL) defect with a corresponding VF defect meet our criteria for parafoveal scotoma (PFS) or peripheral nasal step (PNS). Patients with uveitis or diseases that may affect the peripapillary or macular area, or medication that may influence visual acuity were excluded. When both eyes met the inclusion criteria, one eye per subject was randomly selected for the study.

All patients had performed complete ophthalmic examinations, including slit-lamp biomicroscopy, Goldmann applanation tonometry, gonioscopy, axial length measurement, central corneal thickness measurement, and dilated fundus biomicroscopy. All participants underwent stereoscopic optic disc photography.

Optical Coherence Tomography

Using Cirrus spectral-domain optical coherence tomography (SD-OCT) version 6.0 (Carl Zeiss Meditec, Inc., Dublin, CA, USA), RNFL thickness was determined using optic Disc Cube 200 × 200 scan mode. The Cirrus SD-OCT automatically detects the center of the disc and then draws a circumpapillary circle (radius, 1.73 mm) from the cube data set for RNFL thickness analysis. Poor-quality images with a signal strength less than 6, misalignment, or overt decentration of the measurement circle location, were discarded.

Average (360° measure), superonasal (91°–135°), nasal (136°–225°), inferonasal (226°–270°), inferotemporal (271°–315°), temporal (316°–45°), and superotemporal (46°–90°) RNFL thickness was used in the current study. Retinal nerve fiber layer thickness of each sector was estimated by integrating the clock hour RNFL thickness from the Cirrus OCT.[36] We used these sectors in accordance with the structure–function correspondence map suggested by Garway-Heath et al.[37] (Fig. 1).

VF Testing

All participants performed SAP using 24-2, the SITA standard program with a Humphrey field analyzer (Carl Zeiss Meditec, Inc.). Goldmann size III targets with a diameter of 0.43° was presented for 200 ms. Frequency doubling technology perimetry was performed using the 24-2 strategy with 5° stimuli and a spatial frequency of 0.5 cycles/deg, with temporal frequency of 18 Hz with the FDT Humphrey Matrix (Carl Zeiss Meditec, Inc.). Short-wavelength automated perimetry was examined with the 24-2 SITA program of the Humphrey field analyzer. Each of the blue Goldmann size V targets was displayed on a 100 cd/m^2 yellow background.

In all types of VF testing, the mean deviation (MD) and pattern standard deviation (PSD) were evaluated. On the pattern deviation plot, the percentages of significantly depressed VF points at $P < 0.05$ and $P < 0.01$ were evaluated using SAP, FDT, and SWAP. Not included in the comparison of VF sensitivity were the one central point that was examined only by the FDT but not by SAP or SWAP, and two points just above and below the blind spot. A total of 52 VF points remained for the analysis. In SAP and SWAP, VF sensitivity was evaluated using the dB [10 × log(1/Lambert)] scale in 52 points. In FDT matrix perimetry, sensitivities are expressed as the dB [20 × log(1/Michelson contrast)].[38,39] Global and sectoral MS were evaluated on threshold printout in VF tests. Global MS is calculated as the mean of VF sensitivities in 52 points and sectoral MS as those in the sectors according to the structure–function correspondence map suggested by Garway-Heath et al.[37] (Fig. 1). A reliable test was defined as <15% fixation losses, false-positives, or false-negatives. Most patients had no prior experience of performing VF test.

VF Criteria for PFS and PNS

The PFS and the PNS group were determined by one glaucoma specialist (KIJ) based on pattern deviation probability plots in SITA 24-2 test. A PFS included isolated glaucomatous VF defect within 12 points of a central 10° radius in 1 hemifield (Fig. 1). An isolated glaucomatous VF defect within the nasal periphery outside 10° of fixation in one hemifield is indicated as a PNS. A glaucomatous VF defect was defined as a cluster of three or more points with a P value of <5%, one of which had a P value of <1% on the pattern deviation plot.

Data from subjects with VF defects in the central 10° and peripheral nasal fields, with VF defects other than the central or nasal periphery, or with scotoma in the superior and inferior hemifields, were excluded from analysis.

Statistical Analysis

SPSS software (ver. 17.0; SPSS, Inc., Chicago, IL, USA) was used for statistical analyses.

Differences between the PFS and PNS groups were analyzed by Student's t-test for continuous parameters and the χ^2 test for categorical parameters. Differences between the different VF tests were evaluated by a paired t-test. The relationships between the RNFL thickness and VF sensitivity were evaluated by linear ($y = ax + b$) and nonlinear (second-order polynomial [$y = ax^2 + bx + c$] and logarithmic [$y = a\log(x) + b$]) regression analyses. The goodness-of-fit of regression models was reported as the coefficient of determination, R^2. In all analyses, $P < 0.05$ was taken to indicate statistical significance. In the calculation of univariate correlations, the correction was not performed for multiple comparisons because this study was an explorative trial and to minimize the risk of type II errors.

Results

Data from 34 patients with PFS and 33 with PNS were analyzed after exclusion of 1 patient with uveitis and 2 with unreliable VF

Investigative Ophthalmology & Visual Science

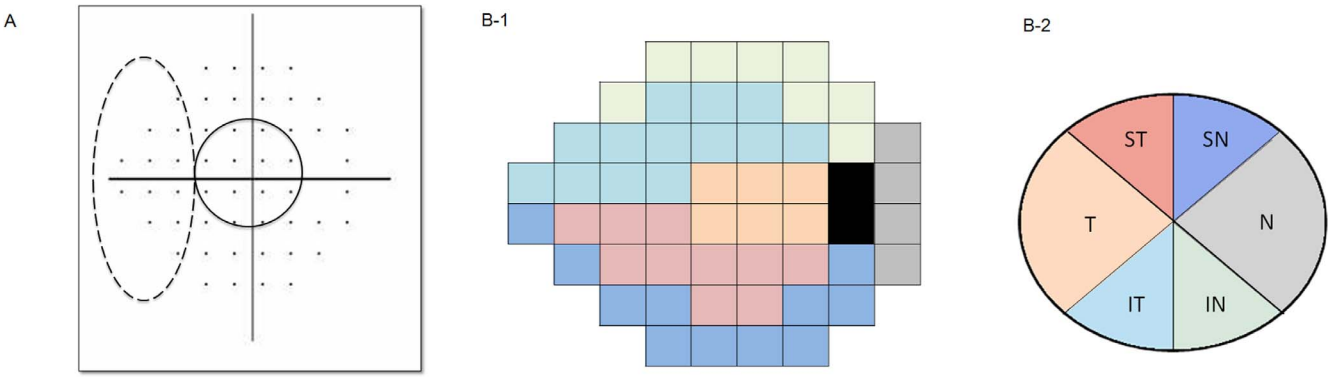

Figure 1. (**A**) Pattern deviation plot divided into two subfields of the Humphrey VF. The parafoveal scotoma group included abnormal points within 12 points of a central 10° radius (*dashed line*). The peripheral nasal step group had abnormal points within 12 nasal peripheral points (*dotted line*) in one hemifield. (**B**) Structure–function correspondence map according to Garway-Heath et al.[18] (**B-1**) Visual field sectors (**B-2**) and peripapillary RNFL thickness. SN, superonasal; N, nasal: IN, inferonasal; IT, inferotemporal; T, temporal; ST, superotemporal.

tests. No significant differences in age, sex, spherical equivalent, and axial length were observed between the PFS and PNS groups ($P = 0.131$, 0.224, 0.192, 0.147, respectively; Table 1). Average RNFL thickness was not significantly different between the two groups ($P = 0.573$). Both groups had similar MD and PSD as evaluated by SAP ($P = 0.331$ and $P = 0.325$, respectively; Table 1).

Comparisons Among SAP, FDT, and SWAP in the PFS and PNS Groups

When the MD was considered, FDT (–7.31 ± 3.88 dB) gave a larger defect than SAP (–2.38 ± 1.38 dB) or SWAP (–5.41 ± 3.06 dB) in the PFS group ($P = 0.043$; Table 2). Pattern standard deviation in FDT was significantly larger than SAP or SWAP in the PNS and PFS groups (all $P < 0.05$).

The mean percentage of the total abnormal points in FDT was significantly greater than those in SAP and SWAP, for 5% and 1% in the PNS group (all $P < 0.001$; Fig. 2). Also in the PFS group, the mean percentage of the total abnormal points in FDT was greater than those in SAP and SWAP, for 5% ($P = 0.005$ and $P < 0.001$, respectively) and 1% (both $P < 0.001$). The mean percentage of the total abnormal points for 5 % and 1% was lesser in the PFS group than the PNS group in all VF tests (all $P < 0.05$).

Overall Structure–Function Relationships

In the PNS group, MD and PSD in the SAP showed significant correlations with average RNFL thickness in linear regression analyses ($r^2 = 0.215$, $P = 0.007$; $r^2 = 0.167$, $P = 0.018$). With regard to FDT, PSD was correlated with average RNFL thickness ($r^2 = 0.137$, $P = 0.034$) in the PNS group. In the PFS group, however, neither MD nor PSD on the SAP showed correlations with the average RNFL thickness ($r^2 = 0.019$, $P = 0.434$ and $r^2 = 0.028$, $P = 0.346$, respectively). In the FDT, MD but not PSD was significantly correlated with the average RNFL thickness in the PFS group ($r^2 = 0.171$, $P = 0.015$ and $r^2 = 0.001$, $P = 0.855$, respectively). Neither MD nor PSD measured by SWAP showed a significant correlation with the average RNFL thickness in either the PNS or PFS group.

In the total patient population, linear regression analyses showed a significant relationship between the average RNFL thickness and global MS (dB) in SAP and FDT ($r^2 = 0.112$, $P = 0.006$ and $r^2 = 0.142$, $P = 0.002$, respectively), but not in SWAP ($r = 0.043$, $P = 0.094$). The similar results were observed in nonlinear regression analyses. In the PNS group, there was a significant relationship between the average RNFL thickness and the global MS in SAP (linear, $r^2 = 0.137$, $P = 0.034$; logarithmic, $r^2 = 0.131$, $P = 0.038$; Table 3; Fig. 3). In the PFS group, however, no significant correlation was observed between the average RNFL thickness and global MS in SAP (linear and nonlinear regression analyses, all $P > 0.05$). With regard to FDT, the relationship between the average RNFL

Table 1. Characteristics of Patients With PFS and PNS

Parameter	PNS Group, $n = 33$	PFS Group, $n = 34$	*P* Value*
Age, y	48.9 ± 11.9	53.5 ± 14.8	0.131
Male/female	20/13	15/19	0.224
Central corneal thickness, μm	545.0 ± 44.0	518.9 ± 62.7	0.055
Spherical equivalent, diopter	−2.4 ± 2.7	−1.5 ± 2.9	0.192
Axial length, mm	25.0 ± 1.3	24.4 ± 1.7	0.147
Average RNFL thickness, μm	76.21 ± 9.31	77.47 ± 8.87	0.573
SAP MD, dB	−2.81 ± 2.16	−2.38 ± 1.38	0.331
SAP PSD, dB	4.79 ± 2.91	4.15 ± 2.30	0.325

* Statistically significant differences between the PFS and PNS groups ($P < 0.05$) by Student's *t*-test for continuous variables or χ^2 test for categorical.

Table 2. Mean Deviation and PSD of FDT and SWAP in PFS and PNS Groups

Parameter	Type of Perimetry	PNS Group, $n = 33$	PFS Group, $n = 34$
MD, dB	SAP	−2.81 ± 2.16	−2.38 ± 1.38
	FDT	−7.57 ± 4.16	−7.31 ± 3.88
	SWAP	−6.98 ± 3.39	−5.41 ± 3.06
	P value		
	SAP vs. FDT	<0.001*	<0.001*
	SAP vs. SWAP	<0.001*	<0.001*
	FDT vs. SWAP	0.459	0.043*
PSD, dB	SAP	4.79 ± 2.91	4.15 ± 2.30
	FDT	6.26 ± 1.38	4.95 ± 1.45
	SWAP	5.34 ± 1.73	4.45 ± 1.68
	P value		
	SAP vs. FDT	<0.001*	0.030*
	SAP vs. SWAP	0.130	0.318
	FDT vs. SWAP	<0.001*	0.042*

* Statistically significant differences among the SAP, FDT, or SWAP ($P < 0.05$) by paired *t*-test.

Investigative Ophthalmology & Visual Science

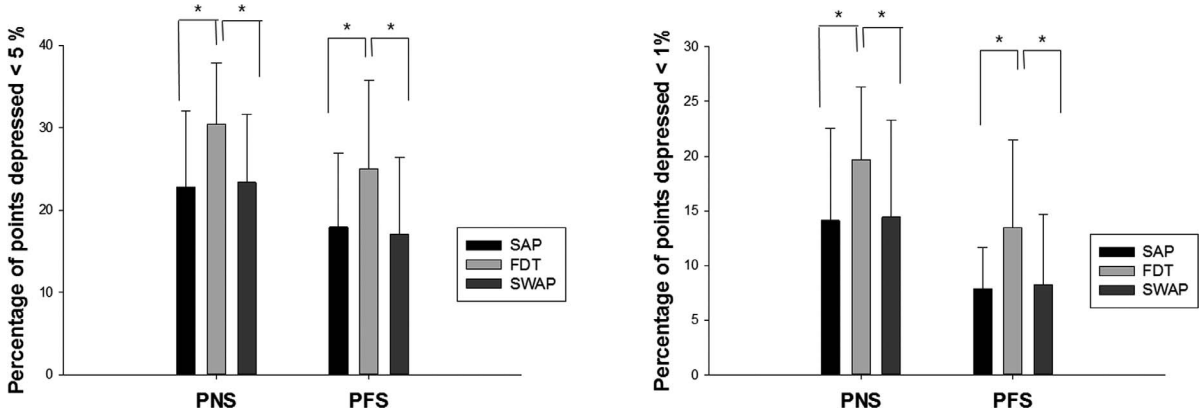

Figure 2. The percentage of total abnormal points among the total VF points significantly depressed <5% and <1% in the pattern deviation plot. The mean percentage of abnormal points in FDT was significantly greater than that in SAP and SWAP, for 5% and 1% in the PNS group (all $P < 0.001$). In the PFS group, the mean percentage of total abnormal points in FDT was greater than the mean percentages of abnormal points in SAP and SWAP, for 5% ($P = 0.005$, $P < 0.001$, respectively) and 1% (both $P < 0.001$).

thickness and overall MS was significant in the PFS group (linear, $r^2 = 0.239$, $P = 0.003$; second-order polynomial, $r^2 = 0.240$, $P = 0.014$; logarithmic, $r^2 = 0.239$, $P = 0.003$). There was no significant correlation between RNFL thickness and global MS for SWAP in all regression analyses ($P > 0.05$).

Topographic Structure–Function Relationships

Table 4 shows the topographic structure–function relationships between RNFL thickness and SAP or FDT, and SWAP parameters in six VF sectors. In the PNS group, superotemporal ($r^2 = 0.300$, $P = 0.001$) and inferotemporal ($r^2 = 0.302$, $P = 0.001$; Fig. 4) RNFL thicknesses showed a linear relationship with the corresponding VF sensitivities in SAP. Significant correlations (r^2) between superotemporal and inferotemporal RNFL thicknesses with regional VF sensitivity were found for FDT and SWAP.

In the PFS group, however, the temporal RNFL thickness of the PFS group was not significantly correlated with the corresponding MS in SAP ($r^2 = 0.103$, $P = 0.065$). With regard to FDT perimetry, the temporal sector showed a linear relationship with the corresponding VF sensitivity ($r^2 = 0.277$, $P = 0.001$). In SWAP, the temporal RNFL thickness was not significantly associated with regional VF sensitivity ($r^2 = 0.052$, $P = 0.192$). Nonlinear regression analyses (second-polynomial and logarithmic regression) showed a similar structure–function relationship to that in the linear regression analyses.

Discussion

We demonstrated that global and sectoral structure–function relationships were comparable among SAP, FDT, and SWAP in glaucoma patients with peripheral scotoma. In glaucoma with PFS, however, the topographic structure–function relationship was poor in SAP or SWAP. The structure–function relationship was favorable with FDT in patients with PFS.

In glaucoma patients with peripheral scotoma, the overall structure–function relationship was similar between SAP and FDT in this study corresponding to the study of Pinto et al.[39] in which correlations between RNFL thickness and MS measured in dB were similar for SAP and the FDT.

In the PFS group, no significant correlation was observed between the average RNFL thickness and overall MS in SAP (linear and nonlinear regression analyses, all $P > 0.05$). In addition, the temporal RNFL thickness of the PFS group showed no significant correlation with the corresponding MS in SAP (linear and nonlinear regression analyses, all $P > 0.05$). Poor correlations were found previously in the temporal sector between RNFL thickness measured using Spectralis OCT and the VF sensitivity measured using SAP in the corresponding area.[39] In one study investigating the structure–function relationship using scanning laser polarimetry and SAP in glaucoma patients, the strongest correlation was shown in the superotemporal sector, followed by inferotemporal sectors, while the temporal sector showed no statistically significant results.[40] In another study evaluating structure–function relationships using SD-OCT, weak correlations were detected between temporal RNFL thickness and the corresponding VF areas.[41] Discrepancies were found among studies evaluating the structure–function relationships in the temporal sector. We assumed that the use of different imaging devices or proportion of PFS patients may affect the structure–function relationship in the temporal sector.

In glaucoma with PFS, FDT performed well in the overall and temporal sector. These findings corresponded to those of Pinto et al.,[39] who reported that temporal RNFL thickness was

Table 3. Structure–Function Relationship Between Global Mean Sensitivity of VF and Average RNFL Thickness

	Linear				Second-Order Polynomial				Logarithmic			
	PNS Group		PFS Group		PNS Group		PFS Group		PNS Group		PFS Group	
Average pRNFLT vs. Global MS	r^2	*P* Value	r^2	*P* Value	r^2	*P* Value	r^2	*P* Value	r^2	*P* Value	r^2	*P* Value
SAP	0.137*	0.034*	0.089	0.086	0.144	0.096	0.136	0.104	0.131*	0.038*	0.101	0.067
FDT	0.076	0.120	0.239*	0.003*	0.076	0.304	0.240*	0.014*	0.076	0.120	0.239*	0.003*
SWAP	0.068	0.142	0.019	0.443	0.088	0.251	0.023	0.692	0.063	0.158	0.017	0.458

* Statistically significant values ($P < 0.05$).

Investigative Ophthalmology & Visual Science

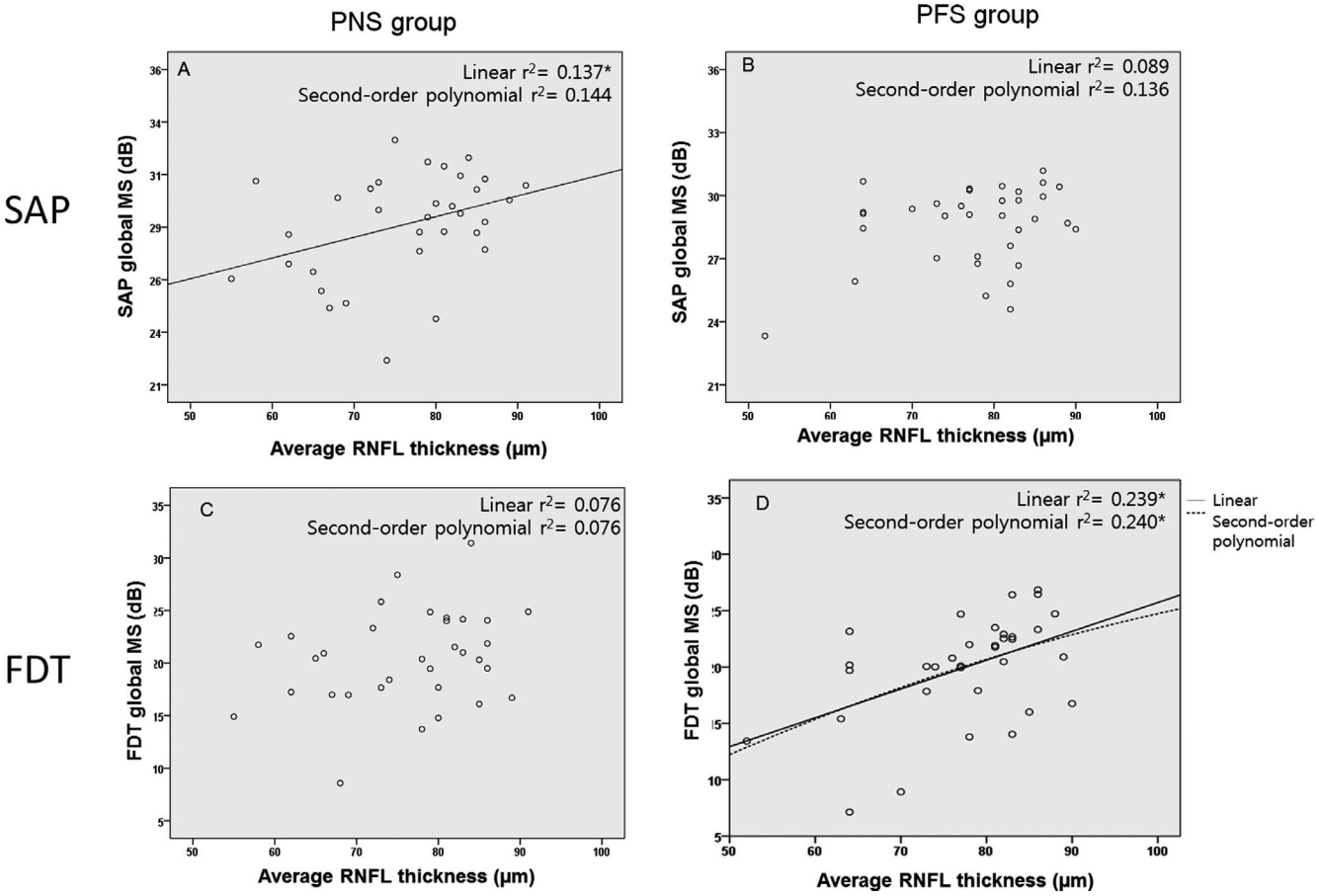

Figure 3. Scatterplots showing the relationships between the global MS (dB) of the VF and average RNFL thickness in patients with the PNS (**A**, **C**) and PFS (**B**, **D**). Global MS was measured by SAP (**A**, **B**) and FDT (**C**, **D**). *Regression analyses with $P < 0.05$.

significantly related to the corresponding VF sensitivity measured using FDT, but not with that using SAP. In another study, temporal RNFL thickness measured by Heidelberg retina tomography (HRT) had a weak correlation with MS in the corresponding VF area in FDT and SAP.[42] This was inconsistent with our findings and may be explained by differences in imaging device and their study population, including patients in the early to advanced stages of glaucoma or different proportion of PFS patients. The strength of the current study is that we observed the structure–function relationship between MS in parafoveal VF area and temporal RNFL sector especially in patients with initial PFS.

The ganglion cell layer is approximately four to six layers thick in the parafoveal region and thins to approximately two cells thick in the peripheral retina.[43] Approximately 50% of the RGCs are placed within 4.5 mm (16°) of the fovea, an area that comprises only 7.3% of the total retina with a peak ganglion density approximately 1 mm from the foveal center.[43] Only four points of the 24-2 VF test fall within the central 8°, the region containing more than 30% of the RGCs.[43,44] Therefore, early RGC loss often occurs in the central macular region, even in patients with VFs classified as normal.[45] By using 24-2 SAP alone, clinicians can miss parafoveal changes occurring before peripheral defects are present.[44] A growing body of evidence suggests that 10-2 VF is more sensitive than 24-2 VF for detecting subtle changes in glaucomatous VF defects within the central 10° because more closely spaced test points are used in 10-2 VF.[44,46] However, 10-2 VF has limitations because it cannot test VF defects outside the central 10°. Thus, more sensitive 24-2 VF tests may be needed to detect paracentral VF defects. We assume that FDT using 24-2 strategy may be helpful not to miss paracentral VF defects.

The favorable performance of FDT in glaucoma patients with PFS with regard to structure–function relationship may be explained by the topography of FDT perimetry. The topography of the FDT fields was considerably flatter than SAP or SWAP fields.[32] In FDT, maintaining VF sensitivities with eccentricity may have a role in presenting the constant structure–function relationship in glaucoma patients with PFS and PNS. There are three other speculations for different structure–function relationship between SAP and FDT. First, SAP with a stimulus of 0.43° may skip a considerable retinal area because test points are spaced 6° apart. FDT with a target of 5° covers a larger area, and is less likely to leave retina untested. Second, Swanson et al.[47] found that sensitivity was higher for the frequency-doubling stimulus than for the size III SAP stimulus for magnocellular cells and parvocellular cells. Higher sensitivity may lead to a good structure–function relationship in FDT. Third, receptive field radii of RGCs become smaller as the degree of eccentricity from fixation decreases.[48] Therefore, VF testing may skip more RGCs in the paracentral retina composed of RGCs with a smaller receptive field. Frequency doubling technology with the larger target covers the greater retinal area with higher sensitivity than SAP. Therefore, the strength of FDT could be maximized in the paracentral retina. The further studies are required to investigate the exact underlying mechanism explaining the

Table 4. Structure–Function Relationship Between Regional VF Sensitivity Measured With SAP or FDT or SWAP and the Corresponding Peripapillary RNFL Thickness

	Linear				Second-Order Polynomial				Logarithmic			
	PNS Group		PFS Group		PNS Group		PFS Group		PNS Group		PFS Group	
SD-OCT Sector	r^2	*P* Value	r^2	*P* Value	r^2	*P* Value	r^2	*P* Value	r^2	*P* Value	r^2	*P* Value
SAP												
Superotemporal	0.300*†	0.001*†	0.212†	0.006†	0.309*†	0.004*†	0.215†	0.023†	0.309*†	0.001*†	0.227†	0.004†
Inferotemporal	0.302*†	0.001*†	0.113	0.052	0.429*†	<0.001*†	0.164	0.062	0.350*†	<.001*†	0.092	0.081
Temporal	0.137†	0.034†	0.103*	0.065*	0.181	0.050	0.130*	0.116*	0.155†	0.023†	0.115*	0.050*
Superonasal	0.054	0.193	0.056	0.179	0.056	0.424	0.099	0.197	0.046	0.229	0.076	0.115
Inferonasal	0.161†	0.021†	0.004	0.737	0.163	0.069	0.010	0.853	0.168†	0.018†	0.011	0.564
Nasal	0.016	0.477	0.008	0.254	0.041	0.535	0.021	0.723	0.017	0.472	0.011	0.558
FDT												
Superotemporal	0.196*†	0.010*†	0.437†	<0.001†	0.257*†	0.012*†	0.504†	<0.001†	0.223*†	0.006*†	0.469†	0.001†
Inferotemporal	0.434*†	<0.001*†	0.250†	0.003†	0.453*†	<0.001*†	0.286†	0.005†	0.398*†	<0.001*†	0.248†	0.003†
Temporal	0.054	0.192	0.277*†	0.001*†	0.185†	0.047†	0.287*†	0.005*†	0.058	0.176	0.286*†	0.001*†
Superonasal	0.018	0.459	0.043	0.237	0.024	0.691	0.089	0.235	0.024	0.394	0.063	0.151
Inferonasal	0.018	0.462	0.039	0.266	0.020	0.742	0.039	0.544	0.020	0.428	0.044	0.232
Nasal	0.180†	0.014†	0.038	0.270	0.252†	0.013†	0.094	0.217	0.171†	0.017†	0.033	0.302
SWAP												
Superotemporal	0.199*†	0.009*†	0.012	0.543	0.201*†	0.035*†	0.039	0.539	0.218*†	0.006*†	0.117	0.511
Inferotemporal	0.244*†	0.003*†	0.157†	0.020†	0.262*†	0.011*†	0.174	0.051	0.233*†	0.004*†	0.137†	0.031†
Temporal	0.074	0.126	0.052*	0.192*	0.086	0.259	0.053*	0.430*	0.086	0.098	0.053*	0.190*
Superonasal	0.030	0.332	0.011	0.551	0.031	0.628	0.012	0.836	0.030	0.332	0.018	0.446
Inferonasal	0.056	0.187	0.015	0.492	0.068	0.348	0.019	0.748	0.067	0.146	0.023	0.393
Nasal	0.006	0.656	0.015	0.484	0.012	0.833	0.020	0.730	0.008	0.615	0.015	0.484

* The cells of each corresponding sector for PNS or PFS.
† Statistically significant values ($P < 0.05$).

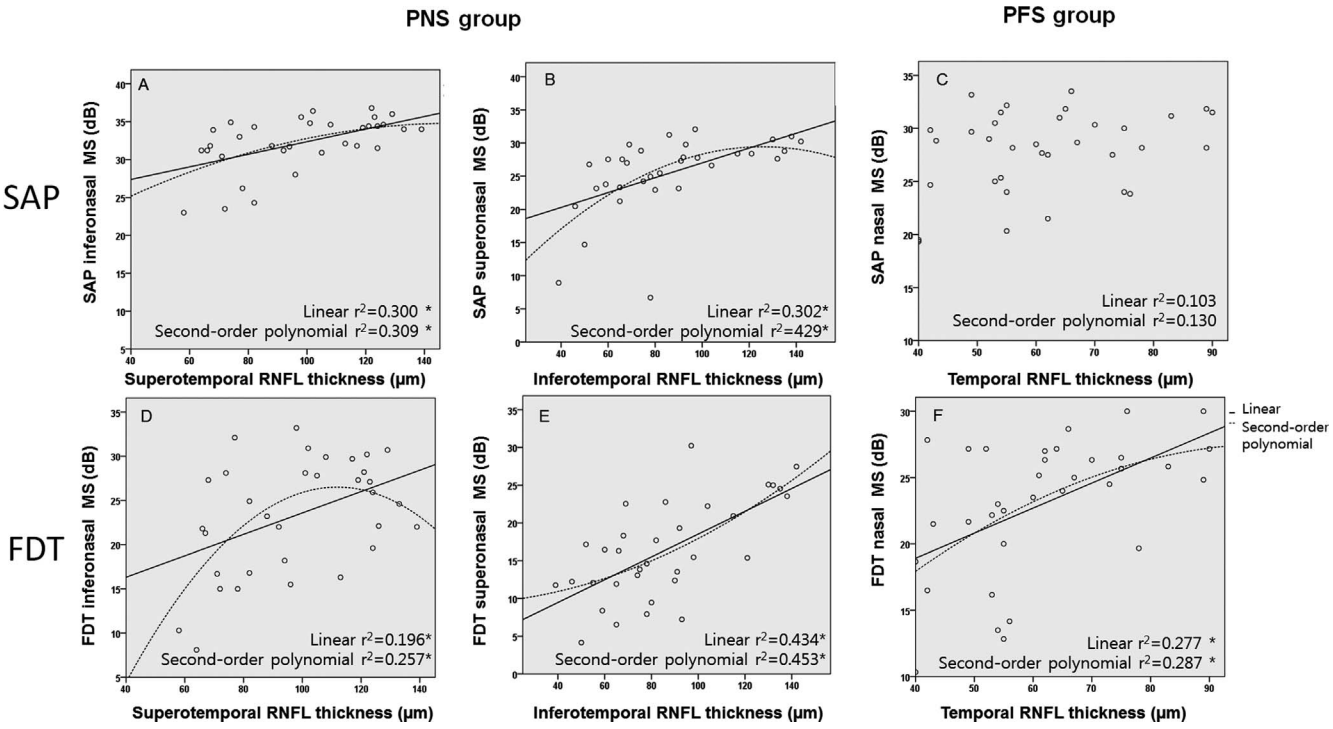

Figure 4. Structure–function relationship between sectoral VF sensitivity (dB) and the corresponding RNFL thickness in patients with the PNS (**A**, **B**, **D**, **E**) and PFS (**C**, **F**). *Regression analyses with $P < 0.05$.

favorable performance of FDT in glaucoma patients with PFS with regard to structure–function relationship.

Short-wavelength automated perimetry is one of the most common VF testing technologies used in clinical practice, along with SAP and FDT perimetry.[15] Yamagishi et al.[49] reported that in 14 patients having open-angle glaucoma with focal optic disc damage, structural damage evaluated with HRT was topographically related to visual loss on blue–yellow perimetry. Other studies indicated relatively good associations between RNFL defects and SWAP abnormalities.[5,50–52] However, the poorer relationship between RNFL thickness and SWAP sensitivity, compared to SAP sensitivity, was observed in some studies.[52,53] We found that SWAP performed relatively well in glaucoma with peripheral scotoma, whereas it did not in that with paracentral scotoma. Our findings were corresponding to the previous study that the structure–function relationship between temporal RNFL thickness and the paracentral VF defects were not significant, although overall RNFL thinning was relatively well correlated with SWAP damage.[52] The topography of SWAP is steeper than corresponding SAP, with VF sensitivity decreasing more rapidly with increasing eccentricity.[32] In SWAP, higher range of VF sensitivities within the tested fields may explain the difference in the structure–function relationship between glaucoma patients with paracentral and peripheral scotoma.

High reliability is one of important elements of good visual function test for glaucoma.[54] Test–retest variability was lower with FDT compared to SAP using size III stimuli.[18–23] These variability properties of FDT could result from increased stimulus size or decreased stimulus range.[18] Test–retest variability of VF by SAP is greater within and near glaucomatous VF defects than to regions with normal sensitivity.[16–18] Increased variability with reductions in sensitivity is not present for frequency-doubling perimetry.[18–23] Good reproducibility for FDT may also have a role in enhancement of structure–function relationships in glaucoma with PFS.[42,54] Short-wavelength automated perimetry had a relatively high degree of variability than that for white-on-white perimetry, such as SAP.[55,56] Less reproducibility of SWAP may be a factor for weak structure–function relationship in glaucoma.

In the PFS group, there were significant correlations between superotemporal or inferotemporal RNFL thickness with regional VF sensitivity for SAP, FDT, and SWAP. Some points in the superotemporal or inferotemporal sector were within 10° in the VF in the structure–function correspondence map (Fig. 1). Parafoveal scotoma may include a part of glaucomatous damage in superotemporal or inferotemporal sector. In addition, glaucomatous damage occurs preferentially in the superotemporal or inferotemporal sectors of the optic nerve head.[42,57–59] That can be one of reasons for significant correlations in superotemporal or inferotemporal sector in glaucoma patients with PFS. Mansoori et al.[60] reported that RNFL thickness measurements for temporal quadrants showed higher variability than superior and inferior quadrants in normal and glaucomatous eyes. Higher variability for temporal RNFL thickness measurements using SD-OCT may contribute to poor structure–function relationship in the temporal sector compared to the superotemporal or inferotemporal sector in patients with PFS.

There are some limitations in the current study. One of them is the relatively small sample size. As far as we know, however, this is the first study to investigate the structure–function relationships with three types of perimetry in glaucoma patients with paracentral and peripheral scotoma. Second, the calculation of stimulus contrast for each perimetry is different. Stimulus contrast was expressed as Weber contrast ($\Delta L/L$) in SAP or SWAP and as Michelson contrast ($Lmax - Lmin/Lmax + Lmin$) in Matrix FDT perimetry.[15] Nevertheless, the comparison between different VF types with currently available techniques may be clinically significant. Third, the structure–function correspondence map suggested by Garway-Heath et al.[37] was used in this study. This map relates VF tests location to regions of the optic disc. Corresponding sectors of the optic disc to VF test points may be changed if a different structure–function model is used. Application of the structure–function map using such as ganglion cell–inner plexiform layer thickness also may lead to different results. Further studies using different structure–function models in glaucoma patients with paracentral scotoma may be helpful.

Because of the clinical significance of central visual disturbance, an accurate assessment of visual function in macular region is important.[33–35] In glaucoma patients with paracentral scotoma, favorable performance of FDT was found with regard to the structure–function relationship, even though good topographic correlations were found in glaucoma with peripheral scotoma using SAP, FDT, or SWAP. Therefore, FDT may be valuable to gain a better understanding of the structure–function relationships, and have a role as an additional tool for evaluation of visual function in glaucoma with paracentral scotoma. Further investigation of progression using FDT may be helpful in cases of glaucoma with PFS.

Acknowledgments

Supported by Basic Science Research Program through the National Research Foundation of Korea (NRF) funded by the Ministry of Education (2014R1A1A2059143). The authors alone are responsible for the content and writing of the paper.

Disclosure: **K.I. Jung**, None; **M.K. Kang**, None; **J.A. Choi**, None; **H.-Y. Shin**, None; **C.K. Park**, None

References

1. Hood DC, Kardon RH. A framework for comparing structural and functional measures of glaucomatous damage. *Prog Retin Eye Res*. 2007;26:688–710.
2. Quigley HA, Addicks EM, Green WR. Optic nerve damage in human glaucoma. III. Quantitative correlation of nerve fiber loss and visual field defect in glaucoma, ischemic neuropathy, papilledema, and toxic neuropathy. *Arch Ophthalmol*. 1982; 100:135–146.
3. Quigley HA, Dunkelberger GR, Green WR. Retinal ganglion cell atrophy correlated with automated perimetry in human eyes with glaucoma. *Am J Ophthalmol*. 1989;107:453–464.
4. Anderson RS. The psychophysics of glaucoma: improving the structure/function relationship. *Prog Retin Eye Res*. 2006;25: 79–97.
5. Fogagnolo P, Rossetti L, Ranno S, Ferreras A, Orzalesi N. Short-wavelength automated perimetry and frequency-doubling technology perimetry in glaucoma. *Prog Brain Res*. 2008; 173:101–124.
6. Brusini P, Salvetat ML, Zeppieri M, Parisi L. Frequency doubling technology perimetry with the humphrey matrix 30-2 test. *J Glaucoma*. 2006;15:77–83.
7. Medeiros FA, Sample PA, Zangwill LM, Liebmann JM, Girkin CA, Weinreb RN. A statistical approach to the evaluation of covariate effects on the receiver operating characteristic curves of diagnostic tests in glaucoma. *Invest Ophthalmol Vis Sci*. 2006;47:2520–2527.
8. Racette L, Medeiros FA, Zangwill LM, Ng D, Weinreb RN, Sample PA. Diagnostic accuracy of the matrix 24-2 and original n-30 frequency-doubling technology tests compared with standard automated perimetry. *Invest Ophthalmol Vis Sci*. 2008;49:954–960.
9. Spry PG, Hussin HM, Sparrow JM. Clinical evaluation of frequency doubling technology perimetry using the Hum-

phrey Matrix 24-2 threshold strategy. *Br J Ophthalmol*. 2005; 89:1031–1035.

10. Sample PA, Medeiros FA, Racette L, et al. Identifying glaucomatous vision loss with visual-function-specific perimetry in the diagnostic innovations in glaucoma study. *Invest Ophthalmol Vis Sci*. 2006;47:3381–3389.
11. Burgansky-Eliash Z, Wollstein G, Patel A, et al. Glaucoma detection with matrix and standard achromatic perimetry. *Br J Ophthalmol*. 2007;91:933–938.
12. Leeprechanon N, Giangiacomo A, Fontana H, Hoffman D, Caprioli J. Frequency-doubling perimetry: comparison with standard automated perimetry to detect glaucoma. *Am J Ophthalmol*. 2007;143:263–271.
13. Tafreshi A, Sample PA, Liebmann JM, et al. Visual function-specific perimetry to identify glaucomatous visual loss using three different definitions of visual field abnormality. *Invest Ophthalmol Vis Sci*. 2009;50:1234–1240.
14. Jampel HD, Singh K, Lin SC, et al. Assessment of visual function in glaucoma: a report by the American Academy of Ophthalmology. *Ophthalmology*. 2011;118:986–1002.
15. Liu S, Lam S, Weinreb RN, et al. Comparison of standard automated perimetry, frequency-doubling technology perimetry, and short-wavelength automated perimetry for detection of glaucoma. *Invest Ophthalmol Vis Sci*. 2011;52:7325–7331.
16. Flammer J, Drance SM, Zulauf M. Differential light threshold. Short- and long-term fluctuation in patients with glaucoma, normal controls, and patients with suspected glaucoma. *Arch Ophthalmol*. 1984;102:704–706.
17. Werner EB, Petrig B, Krupin T, Bishop KI. Variability of automated visual fields in clinically stable glaucoma patients. *Invest Ophthalmol Vis Sci*. 1989;30:1083–1089.
18. Swanson WH, Horner DG, Dul MW, Malinovsky VE. Choice of stimulus range and size can reduce test-retest variability in glaucomatous visual field defects. *Transl Vis Sci Technol*. 2014;3(5):6.
19. Spry PG, Johnson CA, McKendrick AM, Turpin A. Variability components of standard automated perimetry and frequency-doubling technology perimetry. *Invest Ophthalmol Vis Sci*. 2001;42:1404–1410.
20. Chauhan BC, Johnson CA. Test-retest variability of frequency-doubling perimetry and conventional perimetry in glaucoma patients and normal subjects. *Invest Ophthalmol Vis Sci*. 1999;40:648–656.
21. Artes PH, Hutchison DM, Nicolela MT, LeBlanc RP, Chauhan BC. Threshold and variability properties of matrix frequency-doubling technology and standard automated perimetry in glaucoma. *Invest Ophthalmol Vis Sci*. 2005;46:2451–2457.
22. Horani A, Frenkel S, Blumenthal EZ. Test-retest variability in visual field testing using frequency doubling technology. *Eur J Ophthalmol*. 2007;17:203–207.
23. Wall M, Woodward KR, Doyle CK, Artes PH. Repeatability of automated perimetry: a comparison between standard automated perimetry with stimulus size III and V, matrix, and motion perimetry. *Invest Ophthalmol Vis Sci*. 2009;50:974–979.
24. Sample PA, Weinreb RN. Progressive color visual field loss in glaucoma. *Invest Ophthalmol Vis Sci*. 1992;33:2068–2071.
25. Lewis RA, Johnson CA, Adams AJ. Automated perimetry and short wavelength sensitivity in patients with asymmetric intraocular pressures. *Graefes Arch Clin Exp Ophthalmol*. 1993;231:274–278.
26. Johnson CA, Brandt JD, Khong AM, Adams AJ. Short-wavelength automated perimetry in low-, medium-, and high-risk ocular hypertensive eyes. Initial baseline results. *Arch Ophthalmol*. 1995;113:70–76.
27. Girkin CA, Emdadi A, Sample PA, et al. Short-wavelength automated perimetry and standard perimetry in the detection of progressive optic disc cupping. *Arch Ophthalmol*. 2000; 118:1231–1236.
28. Demirel S, Johnson CA. Incidence and prevalence of short wavelength automated perimetry deficits in ocular hypertensive patients. *Am J Ophthalmol*. 2001;131:709–715.
29. Bengtsson B, Heijl A. Normal intersubject threshold variability and normal limits of the SITA SWAP and full threshold SWAP perimetric programs. *Invest Ophthalmol Vis Sci*. 2003;44: 5029–5034.
30. Bengtsson B, Heijl A. Diagnostic sensitivity of fast blue-yellow and standard automated perimetry in early glaucoma: a comparison between different test programs. *Ophthalmology*. 2006;113:1092–1097.
31. Ng M, Racette L, Pascual JP, et al. Comparing the full-threshold and Swedish interactive thresholding algorithms for short-wavelength automated perimetry. *Invest Ophthalmol Vis Sci*. 2009;50:1726–1733.
32. Landers J, Sharma A, Goldberg I, Graham S. Topography of the frequency doubling perimetry visual field compared with that of short wavelength and achromatic automated perimetry visual fields. *Br J Ophthalmol*. 2006;90:70–74.
33. Kolker AE. Visual prognosis in advanced glaucoma: a comparison of medical and surgical therapy for retention of vision in 101 eyes with advanced glaucoma. *Trans Am Ophthalmol Soc*. 1977;75:539–555.
34. Coeckelbergh TR, Brouwer WH, Cornelissen FW, Van Wolffelaar P, Kooijman AC. The effect of visual field defects on driving performance: a driving simulator study. *Arch Ophthalmol*. 2002;120:1509–1516.
35. Fujita K, Yasuda N, Oda K, Yuzawa M. Reading performance in patients with central visual field disturbance due to glaucoma [in Japanese]. *Nippon Ganka Gakkai Zasshi*. 2006;110:914–918.
36. Leite MT, Zangwill LM, Weinreb RN, Rao HL, Alencar LM, Medeiros FA. Structure-function relationships using the cirrus spectral domain optical coherence tomograph and standard automated perimetry. *J Glaucoma*. 2012;21:49–54.
37. Garway-Heath DF, Holder GE, Fitzke FW, Hitchings RA. Relationship between electrophysiological, psychophysical, and anatomical measurements in glaucoma. *Invest Ophthalmol Vis Sci*. 2002;43:2213–2220.
38. Anderson AJ, Johnson CA, Fingeret M, et al. Characteristics of the normative database for the Humphrey matrix perimeter. *Invest Ophthalmol Vis Sci*. 2005;46:1540–1548.
39. Pinto LM, Costa EF, Melo LA Jr, et al. Structure-function correlations in glaucoma using matrix and standard automated perimetry versus time-domain and spectral-domain OCT devices. *Invest Ophthalmol Vis Sci*. 2014;55:3074–3080.
40. Lee PJ, Liu CJ, Wojciechowski R, Bailey-Wilson JE, Cheng CY. Structure-function correlations using scanning laser polarimetry in primary angle-closure glaucoma and primary open-angle glaucoma. *Am J Ophthalmol*. 2010;149:817–825.
41. Aptel F, Sayous R, Fortoul V, Beccat S, Denis P. Structure-function relationships using spectral-domain optical coherence tomography: comparison with scanning laser polarimetry. *Am J Ophthalmol*. 2010;150:825–833.
42. Lamparter J, Russell RA, Schulze A, Schuff AC, Pfeiffer N, Hoffmann EM. Structure-function relationship between FDF, FDT, SAP, and scanning laser ophthalmoscopy in glaucoma patients. *Invest Ophthalmol Vis Sci*. 2012;53:7553–7559.
43. Curcio CA, Allen KA. Topography of ganglion cells in human retina. *J Comp Neurol*. 1990;300:5–25.
44. Traynis I, De Moraes CG, Raza AS, Liebmann JM, Ritch R, Hood DC. Prevalence and nature of early glaucomatous defects in the central 10 degrees of the visual field. *JAMA Ophthalmol*. 2014;132:291–297.
45. Hood DC, Raza AS, de Moraes CG, Johnson CA, Liebmann JM, Ritch R. The nature of macular damage in glaucoma as

Investigative Ophthalmology & Visual Science

revealed by averaging optical coherence tomography data. *Transl Vis Sci Technol*. 2012;1(1):3.

46. Park SC, Kung Y, Su D, et al. Parafoveal scotoma progression in glaucoma: Humphrey 10-2 versus 24-2 visual field analysis. *Ophthalmology*. 2013;120:1546–1550.
47. Swanson WH, Sun H, Lee BB, Cao D. Responses of primate retinal ganglion cells to perimetric stimuli. *Invest Ophthalmol Vis Sci*. 2011;52:764–771.
48. Lee BB. Paths to colour in the retina. *Clin Exp Optom*. 2004; 87:239–248.
49. Yamagishi N, Anton A, Sample PA, Zangwill L, Lopez A, Weinreb RN. Mapping structural damage of the optic disk to visual field defect in glaucoma. *Am J Ophthalmol*. 1997;123: 667–676.
50. Polo V, Abecia E, Pablo LE, Pinilla I, Larrosa JM, Honrubia FM. Short-wavelength automated perimetry and retinal nerve fiber layer evaluation in suspected cases of glaucoma. *Arch Ophthalmol*. 1998;116:1295–1298.
51. Mok KH, Lee VW, So KF. Retinal nerve fiber layer measurement by optical coherence tomography in glaucoma suspects with short-wavelength perimetry abnormalities. *J Glaucoma*. 2003; 12:45–49.
52. Sanchez-Galeana CA, Bowd C, Zangwill LM, Sample PA, Weinreb RN. Short-wavelength automated perimetry results are correlated with optical coherence tomography retinal nerve fiber layer thickness measurements in glaucomatous eyes. *Ophthalmology*. 2004;111:1866–1872.
53. El Beltagi TA, Bowd C, Boden C, et al. Retinal nerve fiber layer thickness measured with optical coherence tomography is related to visual function in glaucomatous eyes. *Ophthalmology*. 2003;110:2185–2191.
54. Johnson CA. The Glenn A. Fry award lecture. Early losses of visual function in glaucoma. *Optom Vis Sci*. 1995;72:359–370.
55. Wild JM. Short wavelength automated perimetry. *Acta Ophthalmol Scand*. 2001;79:546–559.
56. Bengtsson B, Hellgren KJ, Agardh E. Test-retest variability for standard automated perimetry and short-wavelength automated perimetry in diabetic patients. *Acta Ophthalmol*. 2008;86: 170–176.
57. Jonas JB, Gusek GC, Naumann GO. Optic disc morphometry in chronic primary open-angle glaucoma. II. Correlation of the intrapapillary morphometric data to visual field indices. *Graefes Arch Clin Exp Ophthalmol*. 1988;226:531–538.
58. Tuulonen A, Airaksinen PJ. Initial glaucomatous optic disk and retinal nerve fiber layer abnormalities and their progression. *Am J Ophthalmol*. 1991;111:485–490.
59. Jonas JB, Fernandez MC, Sturmer J. Pattern of glaucomatous neuroretinal rim loss. *Ophthalmology*. 1993;100:63–68.
60. Mansoori T, Viswanath K, Balakrishna N. Reproducibility of peripapillary retinal nerve fibre layer thickness measurements with spectral domain optical coherence tomography in normal and glaucomatous eyes. *Br J Ophthalmol*. 2011;95: 685–688.

Investigative Ophthalmology & Visual Science